

Using promoter libraries to reduce metabolic burden due to plasmid-encoded proteins in recombinant *Escherichia coli*

Pasini, Martina; Fernández-castané, Alfred; Jaramillo, Alfonso; De Mas, Carles; Caminal, Gloria; Ferrer, Pau

DOI:
[10.1016/j.nbt.2015.08.003](https://doi.org/10.1016/j.nbt.2015.08.003)

License:
Creative Commons: Attribution-NonCommercial-NoDerivs (CC BY-NC-ND)

Document Version
Peer reviewed version

Citation for published version (Harvard):
Pasini, M, Fernández-castané, A, Jaramillo, A, De Mas, C, Caminal, G & Ferrer, P 2016, 'Using promoter libraries to reduce metabolic burden due to plasmid-encoded proteins in recombinant *Escherichia coli*', *New Biotechnology*, vol. 33, no. 1, pp. 78-90. <https://doi.org/10.1016/j.nbt.2015.08.003>

[Link to publication on Research at Birmingham portal](#)

Publisher Rights Statement:

After an embargo period, this document is subject to the terms of a Creative Commons Non-Commercial No Derivatives license.

Checked October 2015

General rights

Unless a licence is specified above, all rights (including copyright and moral rights) in this document are retained by the authors and/or the copyright holders. The express permission of the copyright holder must be obtained for any use of this material other than for purposes permitted by law.

- Users may freely distribute the URL that is used to identify this publication.
- Users may download and/or print one copy of the publication from the University of Birmingham research portal for the purpose of private study or non-commercial research.
- User may use extracts from the document in line with the concept of 'fair dealing' under the Copyright, Designs and Patents Act 1988 (?)
- Users may not further distribute the material nor use it for the purposes of commercial gain.

Where a licence is displayed above, please note the terms and conditions of the licence govern your use of this document.

When citing, please reference the published version.

Take down policy

While the University of Birmingham exercises care and attention in making items available there are rare occasions when an item has been uploaded in error or has been deemed to be commercially or otherwise sensitive.

If you believe that this is the case for this document, please contact UBIRA@lists.bham.ac.uk providing details and we will remove access to the work immediately and investigate.

Accepted Manuscript

Title: Using promoter libraries to reduce metabolic burden due to plasmid-encoded proteins in recombinant *Escherichia coli*

Author: Martina Pasini Alfred Fernández-Castané Alfonso Jaramillo Carles de Mas Gloria Caminal Pau Ferrer



PII: S1871-6784(15)00149-1
DOI: <http://dx.doi.org/doi:10.1016/j.nbt.2015.08.003>
Reference: NBT 809

To appear in:

Received date: 1-4-2015
Revised date: 31-7-2015
Accepted date: 17-8-2015

Please cite this article as: Pasini, M., Fernández-Castané, A., Jaramillo, A., de Mas, C., Caminal, G., Ferrer, P., Using promoter libraries to reduce metabolic burden due to plasmid-encoded proteins in recombinant *Escherichia coli*, *New Biotechnology* (2015), <http://dx.doi.org/10.1016/j.nbt.2015.08.003>

This is a PDF file of an unedited manuscript that has been accepted for publication. As a service to our customers we are providing this early version of the manuscript. The manuscript will undergo copyediting, typesetting, and review of the resulting proof before it is published in its final form. Please note that during the production process errors may be discovered which could affect the content, and all legal disclaimers that apply to the journal pertain.

Using promoter libraries to reduce metabolic burden due to plasmid-encoded proteins in recombinant *Escherichia coli*

Highlights

- Minimization of the metabolic burden
- Develop of an antibiotic-free expression system, devoid of resistance markers
- Improvement of the recombinant FucA production

Accepted Manuscript

1 **Using promoter libraries to reduce metabolic**
2 **burden due to plasmid-encoded proteins in**
3 **recombinant *Escherichia coli***

4
5
6
7
8 **Martina Pasini**¹, Alfred Fernández-Castané², Alfonso Jaramillo^{3,4}, Carles de Mas¹, Gloria
9 Caminal⁵, Pau Ferrer¹

10 ¹ *Department of Chemical Engineering, Escola d'Enginyeria, Universitat Autònoma de Barcelona,*
11 *Bellaterra (Cerdanyola del Vallès), Spain*

12 ² *School of Chemical Engineering, University of Birmingham, Edgbaston (Birmingham), UK*

13 ³ *School of Life Sciences, University of Warwick, Coventry CV4 7AL, United Kingdom*

14 ⁴ *Institute of Systems and Synthetic Biology, Université d'Évry Val d'Essonne, CNRS, F-91000 Évry,*
15 *France*

16 ⁵ *Institute of Advanced Chemical of Catalonia, IQAC-CSIC, Spain*

17
18
19
20
21 Corresponding autor: Martina Pasini

22 Martina.pasini@uab.cat

23 Tel. +34 93 581 2695

24 Fax. +34 93 581 2013

33 Abstract

34 The over-expression of proteins in recombinant host cells often requires a significant amount of resources
35 causing an increase in the metabolic load for the host. This results in a variety of physiological responses
36 leading to altered growth parameters, including growth inhibition or activation of secondary metabolism
37 pathways. Moreover, the expression of other plasmid-encoded genes such as antibiotic resistance genes
38 or repressor proteins may also alter growth kinetics.

39 In this work, we have developed a second-generation system suitable for *Escherichia coli* expression with
40 an antibiotic-free plasmid maintenance mechanism based on a glycine auxotrophic marker (*glyA*).
41 Metabolic burden related to plasmid maintenance and heterologous protein expression was minimized by
42 tuning the expression levels of the repressor protein (LacI) and *glyA* using a library of promoters and
43 applying synthetic biology tools that allow the rapid construction of vectors. The engineered antibiotic-
44 free expression system was applied to the L-fucose phosphate aldolase (FucA) over-production, showing
45 an increase in production up to 3.8 fold in terms of FucA yield ($\text{mg}\cdot\text{g}^{-1}\text{DCW}$) and 4.5 fold in terms of FucA
46 activity ($\text{AU}\cdot\text{g}^{-1}\text{DCW}$) compared to previous expression. Moreover, acetic acid production was reduced to
47 50%, expressed as $\text{gAc}\cdot\text{gDCW}^{-1}$.

48 Our results showed that the aforementioned approaches are of paramount importance in order to
49 increment the protein production in terms of mass and activity.

50

51

52

53 *Keywords:* Synthetic Biology, Golden Gate Assembly, recombinant protein production and
54 *Escherichia coli*, bioprocess optimization

55

56

57

58

59

60

61

62

63

64

65

66

67

68

69 Introduction

70

71 Among the many systems available, the gram negative bacterium *Escherichia coli* remains one of the most
72 versatile and used host for the production of heterologous proteins, because of its rapid growth rate, the
73 easiness to attain high cell density cultures on inexpensive substrates, its well-characterized genetics and
74 the availability of excellent genetic tools [1]. Efforts in developing strategies to maximize the productivity
75 of recombinant proteins in *E. coli* are well documented in the literature [2] and [3]. Extensive research
76 has been performed over the past years in order to improve recombinant protein production in this cell
77 factory, including the optimization of process parameters such as growth temperature, media
78 composition, induction conditions, as well as engineering novel expression systems [4] and [5].

79 Recent advances in the synthetic biology, allowed the development of new methods and tools to speed
80 up and standardize strain engineering. Compared with conventional DNA cloning protocols, these
81 advanced DNA assembly strategies offer an efficient approach to construct multi-gene pathways in a one-
82 step, scar-less, and sequence-independent manner. In particular, the Parts Registry is a collection of
83 standardized biological parts (BioBricks) that allow the fast assembly of new functions [6], [7] and [8].
84 Individual parts or combinations of parts that encode defined functions can be independently tested and
85 characterized in order to improve the expression system [9]. DNA construction based on the BioBrick
86 theory has become a key part of most metabolic engineering projects and genetic circuits design. The
87 BioBrick concept exploits the advantage that the same promoters, ribosome binding sites, expression
88 tags, antibiotic resistances and origins of replication are frequently reused, with only the genes of interest
89 being varied [7] and [8].

90 Aldolases belong to the class of lyases, which catalyze C-C bond formation leading to enantiomerically
91 pure products, even when the starting materials are non-chiral substrates. In particular, L-Fucose
92 phosphate-aldolase (FucA) catalyzes the reversible reaction of L-fucose-1-phosphate to
93 dihydroxyacetone phosphate (DHAP) and L-lactaldehyde *in vivo*. *E. coli* has been proven to be an efficient
94 platform for soluble overexpression of a wide range of aldolases, both endogenous and from other
95 bacteria [10] and [11].

96 Vidal et al. [12] used rhamnulose 1-phosphate aldolase (RhuA) as a model protein to develop an
97 auxotrophic marker-based expression system consisting of the M15Δ*glyA* strain, with a genome deletion
98 of the *glyA* gene, and a two-plasmid system using the commercial pQE-40 (Qiagen) expression vector,
99 which uses the stronger T5 promoter [13]. The *E. coli glyA* gene encodes for the enzyme serine
100 hydroxymethyl transferase (SHMT), which catalyzes the reversible interconversion between L-threonine
101 and glycine and between serine and glycine [14]. Although previous studies have shown that the
102 auxotrophic *glyA*-based expression vector is a promising alternative approach to the use of antibiotic
103 selection markers [13], increased SMHT levels leads to a metabolic burden, which causes a decrease in
104 activity and specific productivity of recombinant proteins compared to the original system. Besides, the
105 presence of a metabolic load generally brings to a decreased level of energy available for a variety of
106 cellular functions, i.e. for cell maintenance and growth.

107 On the other hand, the use of a two-plasmid expression system often requires the presence of their
108 respective antibiotic markers and this fact is a limitation for the production of certain compounds of
109 pharmaceutical or clinical interest. In our case study, it is of paramount importance to fine-tune the *glyA*
110 and *lacI* expression levels and to eliminate the pREP4 plasmid in order to overcome these limitations and
111 allow the development of an antibiotic-free expression system.

112 In this work, the FucA aldolase has been used as a model protein and its gene (*fucA*) has been firstly
113 cloned into the Qiagen commercial expression system in order to obtain high intracellular expression
114 levels. Secondly, through the application of different synthetic biology approaches, the design and
115 construction of an M15/pQE40-derived expression system consisting of a single vector is presented.
116 Thirdly, the expression levels of the key genes *lacI* and *glyA* have been tuned by the use of different
117 constitutive promoters. Finally, to completely avoid the presence of the antibiotic resistance gene,
118 considered unacceptable in many areas of biotechnology by regulatory authorities [15], the expression
119 system has been further engineered to be finally devoid of antibiotic resistance marker genes and tested
120 for FucA production in shake flasks.

121

122 **Materials and methods**

123

124 **Bacterial strains**

125 The bacterial strain K12-derived *E. coli* M15 (Qiagen) and M15 Δ *glyA* were used for recombinant FucA
126 expression. The strain *E. coli* DH5 α was used for plasmid construction and propagation. The strains were
127 stored at -80°C in cryo-stock aliquots prepared from exponential phase cultures grown in Luria-Bertani
128 (LB) medium. Bacterial strains used in this study are summarized in Table S1 (Supplemented materials).
129 While, abbreviation for all the *E.coli* strains used are summarized in Table S2 (Supplemented materials).

130

131 **Molecular biology techniques**

132 **Plasmid and strain constructions**

133 Plasmid DNA and DNA fragments were isolated or purified using PreYield™ plasmid miniprep system and
134 Wizard® SV gel and PCR clean-up system (Promega) according to the manufacturer's instructions.
135 Restriction enzymes were purchased from Thermo Scientific and T4 DNA ligase from Roche.
136 Transformation of *E. coli* DH5 α , M15 and M15 Δ *glyA* competent cells with the DNA ligation reactions was
137 performed by electroporation using a GenePulser MXcell™ electroporator from Bio-Rad, with a pulse
138 (V=2500v; C=25 μ F; R=200 Ω). Transformants were grown on LB-agar medium or on defined medium
139 (DM)-agar plates supplemented with antibiotic, ampicillin and kanamycin with a final concentration of 100

140 mg-L⁻¹ while the chloramphenicol 30 mg-L⁻¹). Transformant clones were confirmed by colony-PCR, single or
141 double restriction digests and DNA sequencing.

142

143 PCR reactions

144 For fragments up to 2.0 Kb, KOD Polymerase Novagen from Merck Biosciences was used whereas
145 fragments >2.0 Kb, Phusion high-fidelity DNA polymerase (Thermo Scientific) was used, following the
146 guidelines provided by the manufacturer, respectively. For the verification of ligation reactions and
147 transformations, colony PCR was performed using the GoTaq® master mix (Promega). Primers are listed in
148 Table S2 (supplemented materials).

149 Four promoters used (J23117, J23100, J23111 and J23100) in this study and were selected from a
150 combinatorial library of constitutive promoters (Registry for Standard Biological Parts,
151 <http://parts.igem.com>). The strength of the promoters is calculated as the reported activities of red
152 fluorescence protein, being the J23117 the reference promoter, that is, with a given relative transcription
153 efficiency of 1 (in arbitrary units). The promoters J23110, J23111 and J23100 are 5.2, 9.2 and 15.7 fold
154 strongest than J23117, respectively. Each promoter was synthesized by oligonucleotide hybridization
155 including two *Bsa*I sites with 2 different overhangs at both, 5' and 3' terminus.

156 PCR, agarose gel electrophoresis and DNA sequencing were performed to check all the cloning reactions
157 following routine protocols as described in Green and Sambrook [16].

158

159 **Plasmid constructs**

160 Plasmids used in this study are summarized in table S1 (Supplemented materials).

161

162 pQE-FucA

163 The commercial vector pQE-40 (Qiagen) was used as reference vector for the expression of the protein of
164 interest, namely FucA. This expression vector is based on the IPTG-inducible T5 promoter, derived from
165 the T5 phage. This promoter is recognized by *E. coli* RNA polymerase, and has a double *lac* operator (*lac*
166 O) repression module in series to provide tightly regulated and high-level expression of recombinant
167 proteins (Figure S1A). The *fucA* gene was amplified from the pTrc*fuc* vector using the FucA_FW and
168 FucA_REW primers (Supplementary materials table S2). Thereafter, the 0.65 Kbp PCR fragment was
169 digested with the restriction enzymes *Bam*HI and *Hind*III and subsequently cloned into the linearized pQE-
170 40, yielding pQE-FucA (Figure S1B). The final product was then transformed into *E. coli* M15 [pREP4] cells.

171

172 pQE $\alpha\beta$ FucA

173 The DNA fragment comprising the *glyA* gene was amplified from pQE $\alpha\beta$ Rham (designated as
174 $\alpha\beta$ Terminator) [13], including the promoter and the 3' termination region. The resulting 1,784 Kbp

175 fragment was then digested with *BspEI* and *XbaI* and subsequently ligated into pQE-FucA to obtain
176 pQE $\alpha\beta$ FucA (Figure S1C). The ligation reaction was transformed into *E. coli* M15 Δ *glyA*[pREP4].

177

178 BioBrick-based vectors (pSB1C3-J231XX-*lacI-glyA*)

179 The BioBrick vectors were assembled using the golden gate technique [17]. This strategy exploits the ability
180 of type II endonucleases to cleave DNA outside the recognition site leaving an overhang sequence. In this
181 study *BsaI* restriction enzyme and four nucleotide overhangs is used.

182 Both the *lacI* and *glyA* genes were PCR-amplified and were made compatible for the construction of the
183 BioBrick vectors. The *lacI* gene was amplified from the pREP4 plasmid with the GG_*lacI*_FW and
184 GG_*lacI*_REW primers and a *de novo* strong RBS sequence (BBa_B0034,
185 http://parts.igem.org/Part:BBa_B0034) was introduced (Indicated in red in Table S2). The DNA part
186 containing the *glyA* gene was obtained from pQE $\alpha\beta$ Rham using GG_*glyA*_FW and GG_*glyA*_REW primers
187 comprised with a strong RBS sequence (BBa_J61100, http://parts.igem.org/Part:BBa_J61100), being this
188 RBS sequence different to the *lacI* gene in order to avoid homologous recombination (Indicated in green
189 in Table S2). The terminator sequence was maintained from the *glyA* native region, which was PCR-
190 amplified from chromosomal *E. coli* K-12 [13]. *BsaI* sites with two overhangs were introduced at the 5' and
191 3' prime in all assembled fragments to provide directional cloning and to prevent the religation of empty
192 vector. All reaction DNA fragments were prepared equimolar to a concentration of 69 fmol $\cdot\mu$ L⁻¹. To each
193 reaction, 0.5 μ L of *BsaI* and T4 ligase were added. Final reactions were incubated in a thermocycler as
194 follows: 25-30 cycles (37 °C, 3 min; 16 °C, 4 min) and final step 50 °C, 5 min and 80 °C, 5 min. Thus,
195 reactions were performed in one-step restriction-ligation (Figure 1A). Four BioBrick constructs were
196 assembled, each one with a different constitutive promoter to tune the expression levels of *lacI* and *glyA*
197 genes. The four vectors were named pSB1C3-J231XX, where the double X represents the last two digits of
198 the promoter name (Figure 1B). Finally, 2-5 μ L of assembly BioBrick constructs were transformed into 50
199 μ L of *E. coli* DH5 α .

200

201 pQE-FucA_puzzle (J23110)

202 The construction of vector derived from the pQE-FucA and the BioBrick vectors required a two-step
203 assembly. The expression cassette J23110-*lacI-glyA* was amplified from pSB1C3-J23110-*lacI-glyA* using
204 PJ/2_FW and PJ_REW primers. Both, PCR product and destination vector pQE-FucA were digested with
205 *Bpu10I* and *MscI* and subsequently extracted from agarose gel. The expression cassette was cloned into
206 the pQE-FucA (double digested) obtaining the pQE-FucA_puzzle (J23110) (Figure S2A). Finally, the ligation
207 product was transformed into the M15 Δ *glyA* generating M15 Δ *glyA* pQE-FucA_puzzle (J23110), from now
208 on Puzzle strain.

209

210

211

212 pQE-FucA_puzzle (J23110)_Amp^R

213 Vector pQE-FucA_puzzle (J23110) was double digested with *Eco*0109I and *Ahd*I in order to eliminate de
214 *bla* gene. 5'-3' polymerase and 3'-5' exonuclease activities of DNA Polymerase I (Large) Klenow Fragment
215 was used in order to end-removal and fill-in terminal unpaired nucleotides.

216 The blunting DNA reaction, composed of digested vector 0.5 mg, 1 μ L of dNTPS 25 mM (Bioline) and 1 μ L
217 of DNA polymerase I (5U/ μ L) (NEB), was incubated at room temperature (RT) 20 min, followed by a heat
218 inactivation step at 75 °C 10 min. The ligation reaction of the blunt ended DNA fragments and their
219 respective plasmid backbones were carried out at 16 °C overnight using T4 ligase. The resulting ligation
220 (Figure S2B) vector was transformed into *E. coli* M15 Δ *glyA* and plated on defined medium (DM) plates,
221 generating M15 Δ *glyA* pQE-FucA_puzzle (J23110)_ Amp^R, from now on Amp^R strain. Transformants were
222 isolated and tested both, in DM and LB supplemented with ampicillin plates, as a positive and negative
223 control, respectively. Selected transformants were able to grow in defined media but not in LB plates
224 supplemented with ampicillin. Positive clones were validated as described previously.

225

226 Culture media

227 Luria Bertani (LB) medium, containing 10 g·L⁻¹ peptone, 5 g·L⁻¹ yeast extract and 10 g·L⁻¹ NaCl, was used for
228 pre-cultures.

229
230 Defined Medium (DM) used for shake flasks cultures contained per liter: 5 g glucose, 2.97 g K₂HPO₄, 0.60 g
231 KH₂PO₄, 0.46 g NaCl, 0.75 g (NH₄)₂SO₄, 0.11 g MgSO₄·7H₂O, 0.006 g FeCl₃, 0.025 g thiamine, 1.44 g
232 CaCl₂·2H₂O, 0.07 mL·100mL⁻¹ medium of trace elements solution (TES) (TES contained per liter: 0.04 g
233 AlCl₃·6H₂O, 1.74 g ZnSO₄·7H₂O, 0.16 g CoCl₂·6H₂O, 2.18 g CuSO₄·5H₂O, 0.01 g H₃BO₃, 1.42 g MnCl₂·6H₂O,
234 0.01 g NiCl₂·6H₂O, 0.23 g Na₂MoO₄·5H₂O). Agar plates prepared with DM contained 1.5% Agarose.

235 Stock solutions of kanamycin and chloramphenicol were prepared with a concentration of 100 mg·mL⁻¹
236 and 30 mg·mL⁻¹, respectively, and stored at -20 °C. Ampicillin 100 mg·L⁻¹ ethanol stock was prepared and
237 stored at -20 °C. IPTG stock was prepared at 100 mM, and stored at -20 °C.

238 Vitamins, antibiotics, TES, FeCl₃, MgSO₄·4H₂O, CaCl₂·2H₂O and inducer were sterilized by filtration (0.2 μ m
239 syringe filter made from a blend of cellulose esters, Sartorius). Glucose and saline solutions were
240 separately sterilized by autoclaving at 121°C for 30 min.

241

242 Cultivation conditions

243 Pre-inoculum

244 Cryo-stocks stored at -80°C, were use to inoculate Falcon tubes with 15 mL of LB medium supplemented
245 with the corresponding antibiotic if necessary. Growth was performed overnight at 37 °C with agitation.

246 Cultures

247 Three mL of overnight pre-inoculum were transferred into shake flasks containing 100 mL of DM,
 248 following the same growing conditions as pre-inoculum cultures. All cultivations were performed in a
 249 working volume of 100 mL in 500 mL volume-baffled shake flasks. To induce *fucA* expression, IPTG was
 250 added to a final concentration of 1 mM, when an OD₆₀₀ of 1.5 was reached. The induction was maintained
 251 for 4 hours, sampling before induction and 1, 2 and 4 hours after induction.

252

253 Analytical methods

254 Cell concentration was determined by optical density (OD₆₀₀) measurements at 600 nm using a
 255 spectrophotometer (Uvicon 941 Plus, Kontrol). OD values were converted to biomass concentration
 256 expressed as Dry Cell Weight (DCW), being 1 OD₆₀₀ equivalent to 0.3 gDCW·L⁻¹ [18].

257

258 Glucose and acetate concentration were analysed in the broth. One milliliter of culture medium was
 259 separated from biomass by centrifugation at 14.000 rpm 6 min and filtered (0.45 µm membrane filter of
 260 cellulose esters, Millipore) prior to analysis. Glucose concentration was determined enzymatically on an
 261 YSI 2070 system (Yellow Spring System). Acetic acid was analyzed by HPLC (Hewlett Paackard 1050)
 262 equipped with an ICsep COREGEL 87H3 ICE-99-9861 (Transgenomic) column and IR detector (HP 1047),
 263 using 6 M H₂SO₄ (pH 2.0) as mobile phase, flow rate of 0.3 ml·min⁻¹, at 40 °C.

264 The biomass yield, $Y_{X/S}$ was calculated using the following equation:

$$265 \quad Y_{X/S} = \frac{(DCW_{max} - DCW_0)}{(Glc_0 - Glc)} \quad [1]$$

266

267 where, DCW_{max} and DCW_0 (g·L⁻¹) are the maximum and the initial biomass values, respectively. Glc_0 and
 268 Glc_f (g·L⁻¹) are initial and final value of glucose concentration, respectively.

269 The specific substrate uptake rate, q_s , is defined as follows:

$$270 \quad q_s = \frac{\mu}{Y_{X/S}} \quad [2]$$

271

272 where, q_s is given as grams of carbon per grams of biomass per hour (g·g⁻¹DCW·h⁻¹).

273

274 The maximum specific growth rate (μ_{max}) of the different strains is calculated by taking the natural log of
 275 the cell concentration and plotting it over time. The equation [3] shows the relationship between the cell
 276 concentration (X), maximum specific growth rate (μ_{max}) and time (t). Log-linearized Eq. [3] yields a linear
 277 relationship where the μ_{max} is represented by the slope of the linear portion in the plot of the natural log
 278 of cell concentration versus time.

279

$$280 \quad X_t = X_0 \cdot e^{\mu_{max} \cdot t} \quad [3]$$

281 $\ln X_t = \ln X_0 + \mu_{max} \cdot t$ [4]

282 where, X_t and X_0 are, in the linear zone, the OD600 or the cell concentration at any time (t) and at the
283 beginning, respectively.

284

285 **FucA quantification**

286 Samples from culture broths were withdrawn, adjusted to a final OD₆₀₀ of 3, centrifuged and then
287 processed as previously described [19] and [13]. Briefly, pellets were resuspended in 100 mM TrisHCl (pH
288 7.5). Cell suspensions were placed in ice and sonicated over four pulses of 15 seconds each at 50W with 2
289 minutes intervals in ice between each pulse, using a Vibracell™ model VC50 (Sonics & Materials). Cellular
290 debris were then removed by centrifugation and the cleared supernatant was collected for FucA analysis.
291 One unit of FucA activity is defined as the amount of enzyme required to convert 1 μmol of fuculose-1-
292 phosphate in DHAP and L-lactaldehyde for minute at 25 °C and pH 7.5 [13]. To quantify the amount of
293 FucA relative to total intracellular soluble proteins, SDS-PAGE and Bradford protein assay were performed
294 Average values were plotted with error bars. The error indicates the confidence interval with a
295 confidential level of 90%.

296

297 **Results**

298

299 **Comparison of FucA expression between M15[pREP4] and M15[pREP4] ΔglyA strain**

300 Preliminary experiments between *E. coli* M15[pREP4] pQE-FucA and *E. coli* M15 ΔglyA [pREP4] pQE $\alpha\beta$ FucA
301 were performed in shake flask cultures in defined media (DM). Figures 2A and 2B compare biomass and
302 FucA production profiles along time, for the M15[pREP4] and the M15 ΔglyA [pREP4] strains, respectively.
303 The reference M15[pREP4] strain presents a slightly higher maximum specific growth rate (μ_{max}) of $0.49 \pm$
304 0.01 h^{-1} compared to $0.44 \pm 0.01 \text{ h}^{-1}$ in M15 ΔglyA [pREP4]. Moreover, Figures 2C and 2D present glucose
305 consumption and acetate production profiles along time, for the M15[pREP4] and the M15 ΔglyA [pREP4]
306 strains, respectively. Substrate uptake rates (q_s) along the induction phase for both strains were
307 calculated, being 0.37 ± 0.04 and $0.50 \pm 0.13 \text{ gGlc}\cdot\text{g}^{-1}\text{DCW}\cdot\text{h}^{-1}$ for the M15[pREP4] and for the
308 M15 ΔglyA [pREP4], respectively. Moreover, whereas the M15[pREP4] strain reached a final production of
309 $181 \pm 5 \text{ mgFucA}\cdot\text{g}^{-1}\text{DCW}$, with an activity of $721 \pm 82 \text{ AU}\cdot\text{g}^{-1}\text{DCW}$, these values were reduced to 67 ± 37
310 $\text{mgFucA}\cdot\text{g}^{-1}\text{DCW}$ $291 \pm 24 \text{ AU}\cdot\text{g}^{-1}\text{DCW}$ respectively, in the M15 ΔglyA [pREP4] strain (Figure 2A-B).

311 Figure 2E and 2F represented the SDS-PAGE for the M15[pREP4] and the M15 ΔglyA [pREP4] strains,
312 respectively. It can be clearly seen an increase in the SHMT band in the M15 ΔglyA [pREP4] strain (Figure

313 2F). Moreover, in Table 1 it can be seen how the SHMT values of the M15 Δ *glyA*[pREP4] strain, being
314 around 90 mgSHMT·g⁻¹DCW, increased comparing with the M15[pREP4] strain, being around 20
315 mgSHMT·g⁻¹DCW.

316

317 **pREP4 elimination**

318 In order to obtain an expression system completely devoid of antibiotic resistance genes, we initially
319 focused on the elimination of the pREP4 plasmid. The objectives were to i) obtain an expression system
320 based on a single plasmid; ii) clone the *lacI* gene from the pREP4 plasmid to the pQE-expression vector.

321 Accordingly, the pREP4 plasmid was eliminated from the M15 Δ *glyA*[pREP4] pQE α β FucA system, obtaining
322 the derived strain M15 Δ *glyA*[A]. Shake flask cultures were performed in defined media supplemented
323 with ampicillin (data not shown). An increase in the basal FucA production was expected, due to the
324 removal of the repressor protein encoded by the *lacI* gene present on the pREP4 plasmid. Strikingly, no
325 FucA production was detected in these cultures. To further understand this effect, the *lacI* gene from the
326 pREP4 was amplified and cloned into the pQE α β FucA plasmid, obtaining the pQE-*lacI*- α β FucA expression
327 vector. Then, shake flask cultures were performed with M15 Δ *glyA*[B] strain harboring this plasmid (data
328 not shown). However, FucA expression was not found. In order to ensure there was no loss of the
329 expression vector from the cells, the plasmid segregational stability was carried out at different cultivation
330 times before and after induction. The experiments confirmed that the M15 Δ *glyA*[B] cells maintained the
331 expression vector and, consequently, the lack of FucA expression was not the result of plasmid loss.

332 As mentioned in the Materials and Methods section, the T5 promoter has a double lac O region in order
333 to guarantee a strong repression under non-induction conditions. The *lac* repressor, encoded by the *lacI*
334 gene, binds very tightly to the promoter and ensures efficient repression of the strong T5 promoter
335 interfering with the transcription of the gene of interest. In order to further understand whether the
336 promoter leakiness in the absence of repressor is due to structural instability, T5 promoter region isolated
337 from several non-producing M15 Δ *glyA*[A] constructs was sequenced. Interestingly, a deletion in the *lac* O
338 regions was observed, probably due to recombination events in the homology region (data not shown).

339

340 **Tuning of *lacI* and *glyA* expression levels**

341 A series of FucA expressing strains presenting 4 different constitutive transcriptional levels of *lacI* were
342 constructed. Moreover, because the first generation of *glyA*-based auxotrophic system contained the *glyA*
343 gene under the control of the P3 constitutive promoter, resulting in relatively high amounts of its product,
344 the same set of 4 promoters were tested to reduce the transcriptional levels of the *glyA* gene (Vidal L et
345 al., 2008). Thus, an expression cassette was settled where the *lacI* and *glyA* genes were cloned under the
346 control of the four constitutive promoters.

347 The aim was to find the suitable promoter with strength enough to synthesize the minimum amount of
 348 *lacI* inhibitor molecules preventing “promoter leakiness”, as well as the minimal *glyA* transcriptional
 349 levels required to maintain plasmid-bearing cells and optimal cell growth in defined media.

350 The four resulting expression vectors were co-transformed with the pQE-FucA plasmid into M15Δ*glyA*.
 351 The four expression systems generated were named M15Δ*glyA*[C00], [C11], [C10] and [C17] strains.
 352 Biomass and enzyme production were analyzed along time and are presented in Figure 3A, 3B, 3C and 3D,
 353 for M15Δ*glyA*[C00], M15Δ*glyA*[C11], M15Δ*glyA*[C10] and M15Δ*glyA*[C17] strains, respectively.

354 The μ_{\max} measured in the different cultures for the M15Δ*glyA*[C11], M15Δ*glyA*[C10] and M15Δ*glyA*[C17]
 355 transformants were $0.37 \pm 0.01 \text{ h}^{-1}$, $0.48 \pm 0.01 \text{ h}^{-1}$ and $0.41 \pm 0.01 \text{ h}^{-1}$, respectively (Table 2).
 356 M15Δ*glyA*[C00] strain presented significantly higher μ_{\max} being $0.62 \pm 0.05 \text{ h}^{-1}$ (Table 2). The over-
 357 expression of FucA for the 4 selected transformants. The M15Δ*glyA*[C10] results the strain with the higher
 358 production both in term of mass and activity, being $83 \pm 7 \text{ mg}\cdot\text{g}^{-1}\text{DCW}$ and $574 \pm 49 \text{ AU}\cdot\text{g}^{-1}\text{DCW}$,
 359 respectively (Figure 3C).

360 On the other hand, Table 2 and Figure 4 presents the glucose consumption and acetate production
 361 profiles along time for the 4 strains: 4A, 4B, 4C and 4D, for M15Δ*glyA*[C00], M15Δ*glyA*[C11],
 362 M15Δ*glyA*[C10] and M15Δ*glyA*[C17], respectively. It can be observed that the higher q_s value, being $0.79 \pm$
 363 $0.10 \text{ g}\cdot\text{g}^{-1}\text{DCW}\cdot\text{h}^{-1}$, belongs to the M15Δ*glyA*[C00] strain, with an acetate production of $1.50 \pm 0.10 \text{ gAc}\cdot\text{g}^{-1}$
 364 DCW . While the M15Δ*glyA*[C10] strain presents the lower acetate amount of $0.70 \pm 0.12 \text{ gAc}\cdot\text{g}^{-1}\text{DCW}$.

365

366 Expression vector optimization

367 The M15Δ*glyA*[C11] was previously selected as the strain with highest FucA production and specific
 368 activity among the 4 different constructs. To further optimize the expression system, the next goal was
 369 the construction of a single vector harboring both the *fucA* gene under control of the inducible T5
 370 promoter and the *lacI-glyA* cassette cloned under the J23110 constitutive promoter. Such plasmid was
 371 constructed as described in Materials and Methods section and transformed into M15Δ*glyA*, yielding *E.*
 372 *coli* M15Δ*glyA* pQE-FucA_puzzle (J23110) from now on Puzzle strain.

373 The μ_{\max} of the Puzzle strain was $0.45 \pm 0.01 \text{ h}^{-1}$. Maximum FucA mass and FucA specific activity reached
 374 were $162 \pm 7 \text{ mg}\cdot\text{g}^{-1}\text{DCW}$ and $984 \pm 35 \text{ AU}\cdot\text{g}^{-1}\text{DCW}$, respectively (Figure 5A). Besides, the amount of
 375 acetate production for the Puzzle strain results $0.42 \pm 0.03 \text{ g}\cdot\text{g}^{-1}\text{DCW}$.

376 Furthermore, in Table 1, SHMT values are presented, being 66 ± 17 , 62 ± 10 , 54 ± 14 and 54 ± 7
 377 $\text{mgSHMT}\cdot\text{g}^{-1}\text{DCW}$, for the PI, 1h, 2h and 4h induction samples, respectively.

378

379 Development of an antibiotic-free plasmid maintenance

380 Lastly, an expression system completely devoid of antibiotic resistance genes was constructed by
 381 removing the *bla* gene from the expression vector (Figure S2B). The corresponding strain was named *E.*
 382 *coli* M15 Δ *glyA* pQE-FucA_puzzle (J23110)_AmpR-, so-called AmpR- strain.

383 Shake flasks cultures were performed in fined medium (DM) without any antibiotic supplementation. The
 384 time-profiles of the biomass, glucose consumption, acetate and FucA (mass and specific activity) were
 385 analyzed. Results are presented in Figure 6. The μ_{\max} was calculated being μ_{\max} $0.41 \pm 0.01 \text{ h}^{-1}$. In terms of
 386 FucA production, the point of maximum activity corresponds to $1309 \pm 42 \text{ AU}\cdot\text{g}^{-1}\text{DCW}$ with a production
 387 in mass of $219 \pm 5 \text{ mgFucA}\cdot\text{g}^{-1}\text{DCW}$ after 4 h of induction (Figure 6A). Finally, SHMT values were calculated
 388 for each time point of induction. The results are presented in Table 1, where the pre induction sample
 389 with $53 \pm 1 \text{ mgSHMT}\cdot\text{g}^{-1}\text{DCW}$ represents the sample with the higher amount of SHMT.

390

391 Discussion

392

393 In the present work, we have further developed a novel expression system based on an antibiotic-free
 394 plasmid maintenance mechanism. Our stepwise design approach resulted in increased production levels,
 395 up to 3.8-fold in terms of FucA yield ($\text{mg}\cdot\text{g}^{-1}\text{DCW}$) and 4.5-fold in terms of FucA activity ($\text{AU}\cdot\text{g}^{-1}\text{DCW}$),
 396 compared to the reference M15[pREP4] expression system.

397 The comparison between the reference M15[pREP4] and the M15 Δ *glyA*[pREP4] *E. coli* strains
 398 demonstrated that the later presents slightly lower specific growth rate, decreasing from $0.49 \pm 0.01 \text{ h}^{-1}$,
 399 of the reference strain, to $0.44 \pm 0.01 \text{ h}^{-1}$ of the M15 Δ *glyA*[pREP4] strain. This effect may be caused by the
 400 increase in the metabolic burden due to the maintenance of the expression vector in the M15 Δ *glyA* strain.

401 The presence of the *glyA* gene in the vector results in a higher load of this gene due to the multiple copies
 402 of the plasmid. Furthermore, by comparing the qS values of both strains, it can be clearly seen that the
 403 M15 Δ *glyA*[pREP4] strain showed an increase in the specific glucose uptake rate from 0.37 ± 0.04 to $0.50 \pm$
 404 $0.13 \text{ gGlc}\cdot\text{g}^{-1}\text{DCW}\cdot\text{h}^{-1}$. As a consequence, the M15 Δ *glyA*[pREP4] strain accumulated higher amounts of
 405 acetate throughout, reaching a final concentration of $0.54 \pm 0.03 \text{ g}\cdot\text{L}^{-1}$ as it can be observed in Figure 2D
 406 This results in higher acetate specific production rates. This is coherent with previous studies on acetate
 407 under aerobic conditions, pointing at the unbalance between glycolysis rates and the TCA-cycle limited
 408 capacity of *E. coli* [20]. Furthermore, it has been reported that the recombinant protein production is
 409 significantly reduced by acetate accumulation [21]. Such effect can be observed in this study, were both
 410 FucA activity ($\text{AU}\cdot\text{g}^{-1} \text{DCW}$) and FucA mass ($\text{mg}\cdot\text{g}^{-1}\text{DCW}$) (Figure 2B) decrease more than 50 % when
 411 comparing the M15 Δ *glyA*[pREP4] strain to the reference M15[pREP4] (Figure 2A).

412 Noteworthy, the metabolic burden is caused not only due to the overexpression of the protein of interest
 413 but also to the expression of other plasmid-encoded genes, that is, the *glyA* overexpression may also

414 contribute [22]. In fact, the *glyA* gene encoded in the high-copy plasmid leads to substantially higher
415 amounts of its product (SHMT) accumulated as soluble protein in the cytoplasm, compared to the
416 reference strain containing a single copy of *glyA* in the genome as observed in SDS-PAGE (Figure 2E-F) and
417 in Table 1. The SHMT production ($\text{mgSHMT}\cdot\text{g}^{-1}\text{DCW}$) increased more than 4.5-fold when moving from the
418 M15[pREP4] to the M15 Δ *glyA*[pREP4] strain. This observation suggested that *glyA* overexpression
419 imposed a significant burden to the metabolism of the host cell, thereby affecting negatively *FucA*
420 expression levels and the μ_{max} . These preliminary results suggested the regulation of the *glyA* expression
421 levels as an important parameter to be taken into account for further improvement of the expression
422 system and optimization of protein yields.

423 Interestingly, in this work we report the lack of *FucA* expression in the system with no *lacI* gene. This
424 effect may be related to T5 promoter leakiness in absence of *LacI* repressor protein, leading to plasmid
425 structural instability due to recombination events, as supported by the sequencing data. Alternatively, a
426 possible explanation for the lack of *FucA* expression in the single plasmid system may be that the copy
427 number of the *lacI* gene increases when cloned into the pQE-40 vector, resulting in significantly higher
428 levels of intracellular *LacI*. In fact, the pQE vector is based on the plasmid replication origin ColE1, which
429 presents a copy number 2-fold higher compared with the P15A replicon of pREP4 [1].

430 These experiments confirmed that *glyA* and *lacI* co-expression were required. Fine-tuning the co-
431 expression of the two genes allowed to i) reduce the metabolic burden related to plasmid-encoded
432 proteins and, ii) optimize the regulation and induction of the foreign gene expression, when engineering
433 parts of the reference two-plasmid system into a single plasmid.

434 For this reason, four different expression cassettes were constructed where the *lacI* and *glyA* genes were
435 placed under the control of a set of four constitutive promoters, covering a wide range of transcriptional
436 efficiencies. The resulting selected transformants were named M15 Δ *glyA*[C00], [C11], [C10] and [C17] and
437 tested in triplicate. The specific growth rate measured in the different cultures showed a similar behavior
438 for all the transformants except for those with the J23100 promoter. The strongest promoter, which is the
439 one that presented a μ_{max} 1.3 fold higher than the reference strain M15[pREP4] and the other three
440 strains (Table 2). Conversely, the use of a stronger constitutive promoter for the *lacI* and *glyA* expression
441 such as the J23100 resulted in low detection levels of *FucA*, both, in terms of mass and activity.

442 Therefore, a higher growth rate could be explained as follows: higher constitutive *lacI* expression level
443 may lead to a reduction of the *fucA* expression and subsequently decrease the metabolic burden.
444 Furthermore, when comparing q_s values during the induction phase, it can be clearly seen that the
445 M15 Δ *glyA*[C00] strain shows higher glucose specific uptake rate, being $0.79 \pm 0.10 \text{ g}\cdot\text{g}^{-1}\text{DCW}\cdot\text{h}^{-1}$ (Table 2).
446 Consistently, this strain resulted in the production of the highest yields of acetate, reaching 1.50 ± 0.10
447 $\text{gAc}\cdot\text{g}^{-1}\text{DCW}$.

448 According to the results shown in Figure 3C and Table 2, the selected expression cassette for *lacI* and *glyA*,
449 was the one where both genes were placed under the control of the constitutive promoter J23110. This
450 promoter, which is in the lower range of the tested *lacI* and *glyA* transcriptional levels, seems to down-
451 regulate their transcriptional levels. This suggested that the reduced expression of *lacI* and *glyA*

452 expression seems to have reduced the energy demand and the building blocks necessary for *glyA*
453 synthesis. In addition, T5 promoter leakiness was minimized, resulting in an overall reduced metabolic
454 burden. This result is reflected in the fact that the μ_{\max} of this strain was comparable to that of the
455 M15[pREP4] reference strain ($0.48 \pm 0.01 \text{ h}^{-1}$) under pre-induction conditions. Furthermore, the
456 M15 Δ *glyA*[C10] strain presented the lowest q_s ($0.44 \pm 0.06 \text{ g}\cdot\text{g}^{-1}\text{DCW}\cdot\text{h}^{-1}$) and acetate yields (0.70 ± 0.12
457 $\text{g}\cdot\text{g}^{-1}\text{DCW}$) compared to the other three constructs and the highest FucA production, both in terms of
458 mass, $83 \pm 7 \text{ mg}\cdot\text{g}^{-1}\text{DCW}$ and activity, $574 \pm 49 \text{ AU}\cdot\text{g}^{-1}\text{DCW}$.

459 Interestingly, FucA production values increased even more in the strain Puzzle strain compared to the
460 previous system with two plasmids. In particular, while the μ_{\max} , being $0.45 \pm 0.01 \text{ h}^{-1}$, was still
461 comparable to those from the preceding 2-plasmid construct and original reference strains (being $0.48 \pm$
462 0.01 h^{-1} and $0.49 \pm 0.01 \text{ h}^{-1}$, respectively), the maximum FucA mass and FucA specific activity reached
463 were $162 \pm 7 \text{ mg}\cdot\text{g}^{-1}\text{DCW}$ and $984 \pm 35 \text{ AU}\cdot\text{g}^{-1}\text{DCW}$, respectively (Figure 5A and Table 3). Comparing
464 these values with those obtained with the M15[pREP4] reference strain ($181 \pm 5 \text{ mg FucA}\cdot\text{g}^{-1}\text{DCW}$ and
465 $721 \pm 82 \text{ AU}\cdot\text{g}^{-1}\text{DCW}$), it can be observed how the specific activity increased 1.4-fold even though the
466 amount of the recombinant protein was relatively lower. Besides, the Puzzle strain presented a reduction
467 in the amount of acetate production, being $0.42 \pm 0.03 \text{ g}\cdot\text{g}^{-1}\text{DCW}$, in comparison with the $0.73 \pm 0.04 \text{ g}\cdot\text{g}^{-1}$
468 DCW of the reference strain.

469 These results suggest that transcriptional tuning of *lacI* expression levels is a key factor to improve *fucA*
470 expression regulation, leading to a higher FucA specific activity. Moreover, the tuning of *glyA* levels has a
471 positive effect on the reduction of the metabolic load due to expression of plasmid-encoded genes (also
472 reflected in the reduced acetate production). In fact, SHMT values were almost 50% reduced comparing
473 the Puzzle with the M15 Δ *glyA*[pREP4] strains (Table 1). These results are in accordance with the
474 observation by Mairhofer et al. [23], who demonstrated that the folding machinery is severely
475 overstrained in the plasmid-based expression system compared with the plasmid-free cells due to the
476 different transcriptional profiles.

477 Finally, the complete deletion of the antibiotic resistance gene has been achieved resulting in the Amp^R
478 strain. A slightly decrease in the μ_{\max} , a value of $0.41 \pm 0.01 \text{ h}^{-1}$ was observed compared to the
479 M15[pREP4] and Puzzle strains, which showed a μ_{\max} of $0.49 \pm 0.02 \text{ h}^{-1}$ and $0.45 \pm 0.01 \text{ h}^{-1}$, respectively
480 (Figure 6 and Table 3). This strain presented a significant increase both for the FucA specific mass and
481 FucA specific activity. After 4 h of induction it was found maximum activity that corresponded to $1309 \pm$
482 $42 \text{ AU}\cdot\text{g}^{-1}\text{DCW}$ and $219 \pm 5 \text{ mgFucA}\cdot\text{g}^{-1}\text{DCW}$.

483 Comparing with all the previous constructs, FucA over-production using the antibiotic free-plasmid system
484 is higher than any previous developed system studied. In particular, as it can be seen in Table 3 and in
485 Figure 7, FucA yields in the Amp^R strain is: i) more than 1.2-fold higher comparing with the M15[pREP4]
486 and the Puzzle strains; ii) 2.6-fold higher comparing with the M15 Δ *glyA*[C10] strain and iii) three- fold
487 higher referred to the M15 Δ *glyA*[pREP4] strain. Noteworthy, the FucA activity, in terms of $\text{AU}\cdot\text{g}^{-1}\text{DCW}$,
488 increased through the different stepwise improvements performed along this work. The best performing

489 engineered strain reached 4.5-fold higher values compared to the first M15 Δ *glyA*[pREP4] strain.
490 Additionally, the acetate production, expressed as gAc·gDCW⁻¹, was also significantly reduced.

491

492

493

494 **Conclusions**

495 In this work we have applied rapid assembly strategies for the construction of improved expression
496 systems that are useful for recombinant protein production. Using as a reference expression system
497 commercially available, we have obtained an improved system that resulted in higher protein yields and
498 devoid of antibiotic supply.

499 This case-study demonstrates that tuning the expression levels of *lacI* and *glyA* genes, which encode for
500 the lac repressor and the auxotrophic selection marker protein, respectively, results into a reduction of
501 the metabolic burden leading to a better stability of expression system. This fact allows an improvement
502 of the recombinant protein production due to the alleviation of the metabolic burden and a reduction of
503 acetate secretion. The main advantage of this engineered expression system devoid of antibiotic
504 resistance markers is that it can be used as a platform for the production of a wide range of heterologous
505 proteins where the use of antibiotics is restricted. Our work allows versatile and tuneable levels of
506 expressed proteins at will, and we envisage that it can be potentially used in a wide range of applications
507 and biotechnological processes with a significant reduction of production time and upstream costs.

508 Nonetheless, to broaden the understanding and commercial exploitation using this novel expression
509 platform, studies at bioreactor scale using biomass concentrations comparable to industrial processes
510 should be done.

511

512

513

514

515

516

517

518

519 **Acknowledgements**

520 This work was supported by the Spanish MICINN, project number CTQ2011-28398-CO2-01 and the
521 research group 2009SGR281 and by the Bioprocess Engineering and Applied Biocatalisys Group,
522 department of Chemical Engineering of the Universitat Autònoma de Barcelona, Cerdanyola del
523 Valles (Spain).

524 M. P. acknowledges the Universitat Autònoma de Barcelona for the pre-doctoral fellowship.

525

526

527

528

529 **Ethical statement/conflict of interest**

530 All authors concur with the submission and agree with its publication. The authors declare that they
531 have no conflict of interest.

532 The authors confirm that this work is original and has not been published elsewhere nor is it
533 currently under consideration for publication elsewhere.

534

535 The manuscript does not contain experiments using animals or human studies.

536

537

538 **Authors' contributions**

539 MP: Performed all experiments, acquisition and analysis of all the data, as well as in drafting of the
540 manuscript. AFC: Contributed to the conceptual design of the study and manuscript editing. AJ:
541 Involved in the design of constructs and manuscript edition. CdM, GC and PF: Contributed to the
542 overall conceptual design of the study and data interpretation, as well as in drafting and revision of
543 the manuscript. All Authors read and approved the manuscript.

544

545

546

547

548

549

550

551

552

553 **References**

- 554 [1] Baneyx F. Recombinant protein expression in *Escherichia coli*. *Curr. Opin. Biotechnol* 1999;10:
555 p. 411–421.
- 556 [2] Li M, Wang J, Geng Y, Li Y, Wang Q, Liang Q and Qi Q. A strategy of gene overexpression based
557 on tandem repetitive promoters in *Escherichia coli*. *Microb Cell Fact* 2012;11:19–29.
- 558 [3] Correa A and Oppezzo P. Tuning different expression parameters to achieve soluble
559 recombinant proteins in *E. coli*: Advantages of high-throughput screening. *Biotechnol J*
560 2011;6:715–30.
- 561 [4] Tomohiro M, Skretas G and Georgiou G. Strain engineering for improved expression of
562 recombinant proteins in bacteria. *Microb Cell Fact* 2011;10:32–42.
- 563 [5] Jana S and Deb JK. Strategies for efficient production of heterologous proteins in *Escherichia*
564 *coli*. *Appl Microbiol Biotechnol* 2005;67:289–98.
- 565 [6] Voigt CA. Genetic parts to program bacteria. *Curr Opin Biotechnol* 2006;17, p. 548–557.
- 566 [7] Heinz N and Neumann-Staubitz P. Synthetic biology approaches in drug discovery and
567 pharmaceutical biotechnology. *Appl Microbiol Biotechnol* 2010;87:75–86.
- 568 [8] Vick JE, Johnson ET, Choudhary S, Bloch SE, Lopez-Gallego F, Srivastava P, Tikh IB, Wawrzyn
569 GT and Schmidt-Dannert C. Optimized compatible set of BioBrick™ vectors for metabolic
570 pathway engineering. *Appl Microbiol Biotechnol* 2011;92:1275–1286.
- 571 [9] Yokobayashi Y, Weiss R and Arnold FH. Directed evolution of a genetic circuit. *Appl Biol Sci*
572 2002;99:16587–16591.
- 573 [10] Garcia-junceda E, Gwo-Jenn S, Takeshi S and Wong CH. A New Strategy for the Cloning ,
574 Overexpression and One Step Purification of Three DHAP-Dependent Aldolases: Rhamnulose-
575 1-Phosphate Aldolase, Fucose-1-Phosphate Aldolase and Tagatose-1,6-Diphosphate
576 aldolase. *Biorgan Med Chem* 1995;3:945–953.
- 577 [11] Durany O, de Mas C and López-Santín J. Fed-batch production of recombinant fucose-1-
578 phosphate aldolase in *E. coli*. *Process Biochem* 2005;40:707–716.
- 579 [12] Vidal L, Producción de aldolasas recombinantes : de la biología molecular al desarrollo de
580 procesos. Thesis 2006.
- 581 [13] Vidal L, Pinsach J, Striedner G and Ferrer P. Development of an antibiotic-free plasmid
582 selection system based on glycine auxotrophy for recombinant protein overproduction in
583 *Escherichia coli*. *J Bacteriol* 2008;134:127–13.
- 584 [13] Plamann MD and Stauffer GV. Characterization of the *Escherichia coli* gene for serine
585 hydroxymethyltransferase. *Gene* 1983;22:9–18.
- 586 [14] Glenting J and Wessels S. Ensuring safety of DNA vaccines. *Microb Cell Fact* 2005;4:26.
- 587 [15] Green MR and Sambrook J. *Molecular Cloning* 2012;1.
- 588 [16] Engler C, Kandzia R and Marillonnet S. A one pot, one step, precision cloning method with
589 high throughput capability. *PLoS One* 2008;3:1–9.

- 590 [17] Pinsach J, de Mas C and López-Santín J. Induction strategies in fed-batch cultures for
591 recombinant protein production in *Escherichia coli*: Application to rhamnulose 1-phosphate
592 aldolase. *Biochem Eng J* 2008;41:181-187.
- 593 [18] Vidal L, Durany O, Suau T, Ferrer P and Caminal G. High-level production of recombinant His-
594 tagged rhamnulose 1-phosphate aldolase in *Escherichia coli*. *J Chem Technol Biotechnol*
595 2003;78:1171-1179.
- 596 [19] Jensen EB and Carlsen S. Production of Recombinant Hum an Growth Hormone in *Escherichia*
597 *coli*: Expression of Different Precursors and Physiological Effects of Glucose , Acetate, and
598 Salts. *Biotechnol Bioeng* 1990;36:1-11.
- 599 [20] Lee SY. High cell-density culture of *Escherichia coli*. *Trends in biotechnology* 1996;14:p. 98-
600 105.
- 601 [21] Glick BR. Metabolic Load and heterologous Gene Expression. *Biotechnol Adv* 1995;13:247-
602 261.
- 603 [22] Mairhofer J, Scharl T, Marisch K, Cserjan-Puschmann M and Striedner G. Comparative
604 Transcription Profiling and In-Depth Characterization of Plasmid-Based and Plasmid-Free
605 *Escherichia coli* Expression Systems under Production Conditions. *Appl Environ Microbiol*
606 2013;79:3802-3813.
- 607
- 608
- 609
- 610
- 611
- 612
- 613
- 614
- 615
- 616
- 617
- 618
- 619
- 620
- 621
- 622

623 Figure Legends

624

625 **Fig. 1** Golden Gate Assembly Method. **A)** Schematic diagram of Golden Gate assembly method to
 626 facilitate the construction of the new BioBrick vectors. **C)** Representation of the four pSB-J231XX
 627 vectors, each one with one of the four constitutive promoters. J231XX, constitutive promoter where
 628 the double X represents the last two digits of the promoter name (J23100, J23111, J23110 and
 629 J23117); RBS, ribosome binding site (purple for the *lacI* gene and pink for the *glyA* gene); *lacI*, *lacI*
 630 gene; *glyA*, *glyA* gene; term, termination sequence for the *glyA* gene; *camR*, chloramphenicol
 631 resistance gene; pMB1, replication origin.

632 **Fig. 2 A, B, C and D** represent the profiles along time of shake flasks cultures performed per triplicate
 633 in DM media at 37°C with agitation. (○) Biomass DCW ($\text{g}\cdot\text{L}^{-1}$), (▲) enzyme activity ($\text{AU}\cdot\text{gDCW}^{-1}$), (■)
 634 specific mass production content ($\text{mgFucA}\cdot\text{gDCW}^{-1}$), (▼) Glucose ($\text{g}\cdot\text{L}^{-1}$) and (●) Acetic Acid ($\text{g}\cdot\text{L}^{-1}$). The
 635 arrow indicates the IPTG pulse for the induction. **E and F** represent the SDS-PAGE of shake flasks
 636 culture's samples, where Lane M: molecular weight marker. 1, 2, 3 correspond to the shake flask
 637 culture replicates while the PI (pre induction) and 1 h, 2h and 4h correspond to the time after
 638 induction. The 26 kDa FucA and 46 kDa SHMT bands are indicated in the Figure. **A, C and E** refer to the
 639 M15[pREP4] strain while **B, D and F** refer to the M15 Δ *glyA*[pREP4] strain.

640 **Fig. 3.** (○) Biomass DCW($\text{g}\cdot\text{L}^{-1}$), (▲) enzyme activity ($\text{AU}\cdot\text{g}^{-1}\text{DCW}$) and (■) specific mass production
 641 ($\text{mgFucA}\cdot\text{g}^{-1}\text{DCW}$) profiles along time in defined media at 37°C with agitation of the 4 different
 642 transformants: **A)** M15 Δ *glyA*[00] **B)** M15 Δ *glyA*[11] **C)** M15 Δ *glyA*[10] **D)** M15 Δ *glyA*[17]. The arrow
 643 indicates the IPTG pulse for the induction.

644 **Fig. 4** (▼) Glucose ($\text{g}\cdot\text{L}^{-1}$) and (●) Acetic Acid ($\text{g}\cdot\text{L}^{-1}$) profiles along time in defined media shake flasks
 645 cultures performed per triplicate in DM media at 37°C with agitation of the 4 different transformants:
 646 **A)** M15 Δ *glyA*[00] **B)** M15 Δ *glyA*[11] **C)** M15 Δ *glyA*[10] **D)** M15 Δ *glyA*[17]. The arrow indicates the IPTG
 647 pulse for the induction.

648 **Fig. 5 A)** (○) Biomass DCW ($\text{g}\cdot\text{L}^{-1}$), (▲) enzyme activity ($\text{AU}\cdot\text{g}^{-1}\text{DCW}$), (■) specific mass content
 649 ($\text{mgFucA}\cdot\text{g}^{-1}\text{DCW}$) and **B)** (▼) Glucose ($\text{g}\cdot\text{L}^{-1}$) and (●) Acetic Acid ($\text{g}\cdot\text{L}^{-1}$) profiles, along time in a defined
 650 medium shake flasks cultures performed at 37°C for the Puzzle strain. The arrow indicates the 1mM
 651 IPTG pulse for the induction.

652 **Fig. 6 A)** (○) Biomass DCW($\text{g}\cdot\text{L}^{-1}$), (▲) enzyme activity ($\text{AU}\cdot\text{g}^{-1}\text{DCW}$), (■)specific mass ($\text{mgFucA}\cdot\text{g}^{-1}\text{DCW}$)
 653 and **B)** (▼) Glucose ($\text{g}\cdot\text{L}^{-1}$) and (●) Acetic Acid ($\text{g}\cdot\text{L}^{-1}$) profiles, along time in a defined medium shake
 654 flasks cultures performed at 37°C 150 rpm for the AmpR- strain. The arrow indicates the IPTG pulse for
 655 the induction.

656

657 **Fig. 7 A)** Maximum enzyme activity ($\text{AU}\cdot\text{g}^{-1}\text{DCW}$) and **B)** Maximum specific mass ($\text{mgFucA}\cdot\text{g}^{-1}\text{DCW}$)
 658 along the induction phase for the principal strains presented along this study. A dash-dot line indicates
 659 the value of the M15[pREP4] reference strain.

660

661

662

663

664

665 Table 1 SHMT production ($\text{mg}\cdot\text{g}^{-1}\text{DCW}$) along the induction phase for the principal strains
 666 presented along this study. PI (pre induction) and 1 h, 2h and 4h correspond to the time after
 667 induction.

	M15[pREP4]	M15 Δ glyA[pREP4]	Puzzle	AmpR-
PI	27 \pm 14	92 \pm 14	66 \pm 17	53 \pm 1
1h	14 \pm 1	95 \pm 7	62 \pm 10	44 \pm 11
2h	12 \pm 4	91 \pm 11	54 \pm 14	48 \pm 6
4h	13 \pm 1	90 \pm 14	54 \pm 7	50 \pm 10

668

669 Table 2 Maximum specific growth rate (μ_{max} h^{-1}), FucA activity ($\text{AU}\cdot\text{g}^{-1}\text{DCW}$), FucA mass ($\text{mg}\cdot\text{g}^{-1}$
 670 DCW), q_s of the induction phase and the maximum acetate yield ($\text{g}\cdot\text{g}^{-1}\text{DCW}$) for each of the four
 671 selected transformants M15 Δ glyA[C00], M15 Δ glyA[C11], M15 Δ glyA[C10] and M15 Δ glyA[C17]. The
 672 values represent the sample after 2 hour of induction.

673

Transformant	μ_{max} (h^{-1})	FucA Activity ($\text{AU}\cdot\text{g}^{-1}\text{DCW}$)	FucA mass ($\text{mg}\cdot\text{g}^{-1}\text{DCW}$)	q_s ($\text{g}\cdot\text{g}^{-1}\text{DCW}\cdot\text{h}^{-1}$)	Acetate yield ($\text{g}\cdot\text{g}^{-1}\text{DCW}$)
M15 Δ glyA[C00]	0.62 \pm 0.05	131 \pm 35	22 \pm 9	0.79 \pm 0.10	1.50 \pm 0.10
M15 Δ glyA[C11]	0.37 \pm 0.01	233 \pm 7	66 \pm 4	0.42 \pm 0.09	1.12 \pm 0.09
M15 Δ glyA[C10]	0.48 \pm 0.01	574 \pm 49	83 \pm 7	0.44 \pm 0.06	0.70 \pm 0.12
M15 Δ glyA[C17]	0.41 \pm 0.01	194 \pm 24	50 \pm 5	0.58 \pm 0.01	1.11 \pm 0.05

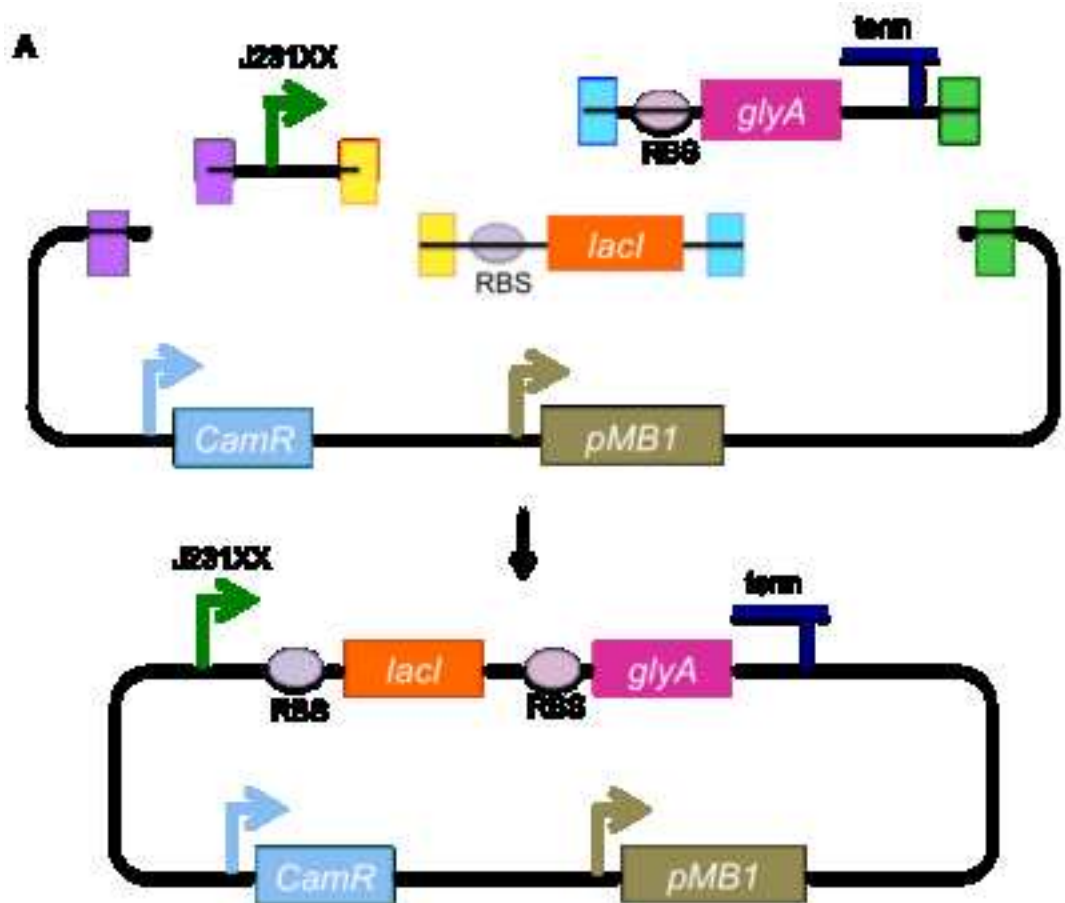
674

675

676 Table 3 Maximum FucA activity ($\text{AU}\cdot\text{g}^{-1}\text{DCW}$), maximum FucA mass ($\text{mg}\cdot\text{g}^{-1}\text{DCW}$), μ_{max} and maximum
 677 acetate yield ($\text{g}\cdot\text{g}^{-1}\text{DCW}$) along the induction phase for the principal strains presented along this
 678 study.

<i>E. coli</i> strains	μ_{max} (h^{-1})	FucA activity ($\text{AU}\cdot\text{g}^{-1}\text{DCW}$)	FucA mass ($\text{mg}\cdot\text{g}^{-1}\text{DCW}$)	Acetate yield ($\text{g}\cdot\text{g}^{-1}\text{DCW}$)
M15[pREP4]	0.49 \pm 0.02	721 \pm 82	181 \pm 5	0.73 \pm 0.04
M15 Δ glyA[pREP4]	0.44 \pm 0.01	291 \pm 24	67 \pm 37	0.90 \pm 0.04
M15 Δ glyA [C10]	0.48 \pm 0.02	574 \pm 49	83 \pm 7	0.70 \pm 0.12
Puzzle	0.45 \pm 0.01	984 \pm 35	162 \pm 7	0.42 \pm 0.03
AmpR ⁻	0.41 \pm 0.01	1309 \pm 42	219 \pm 5	0.37 \pm 0.01

679



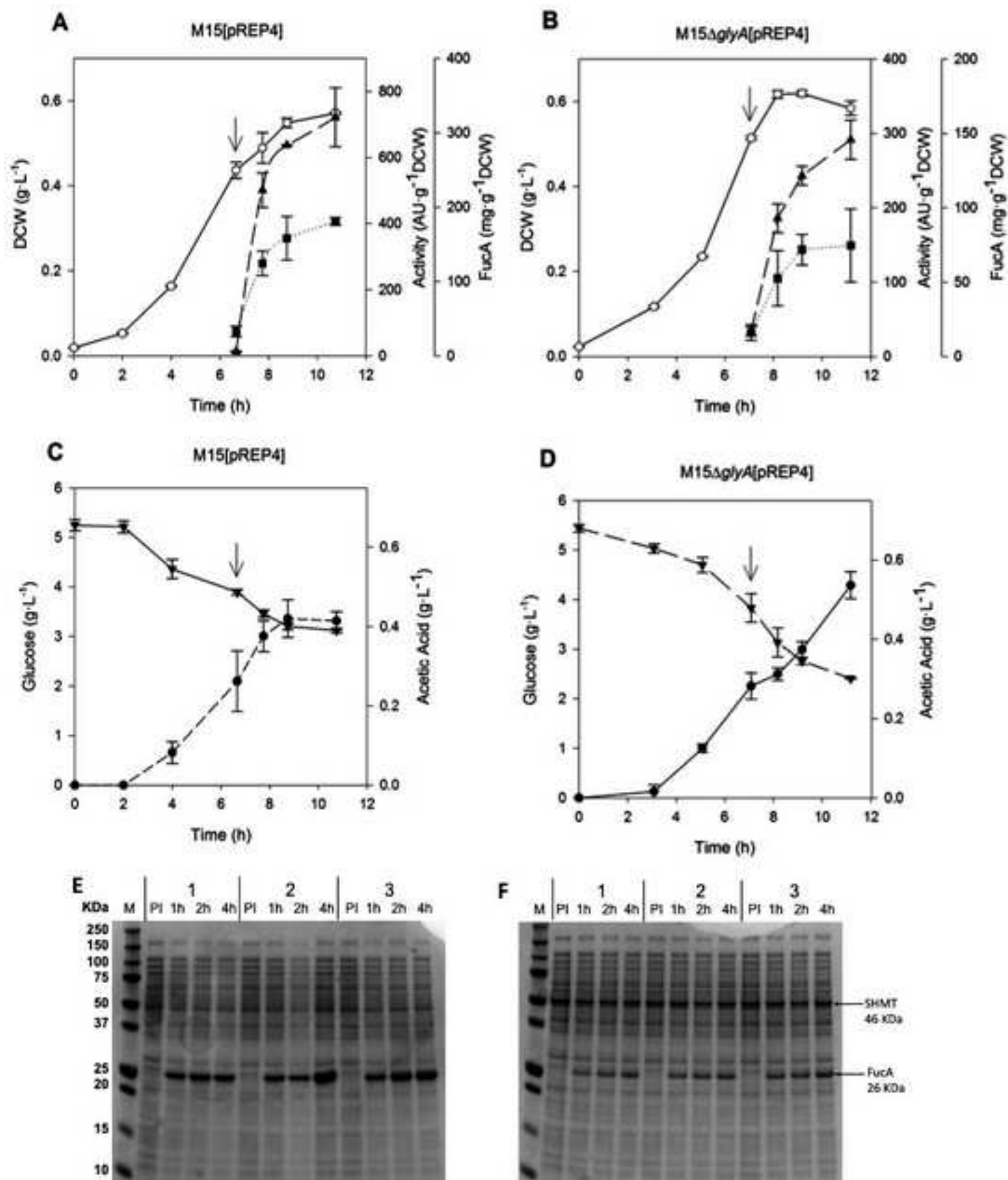


Figure 3

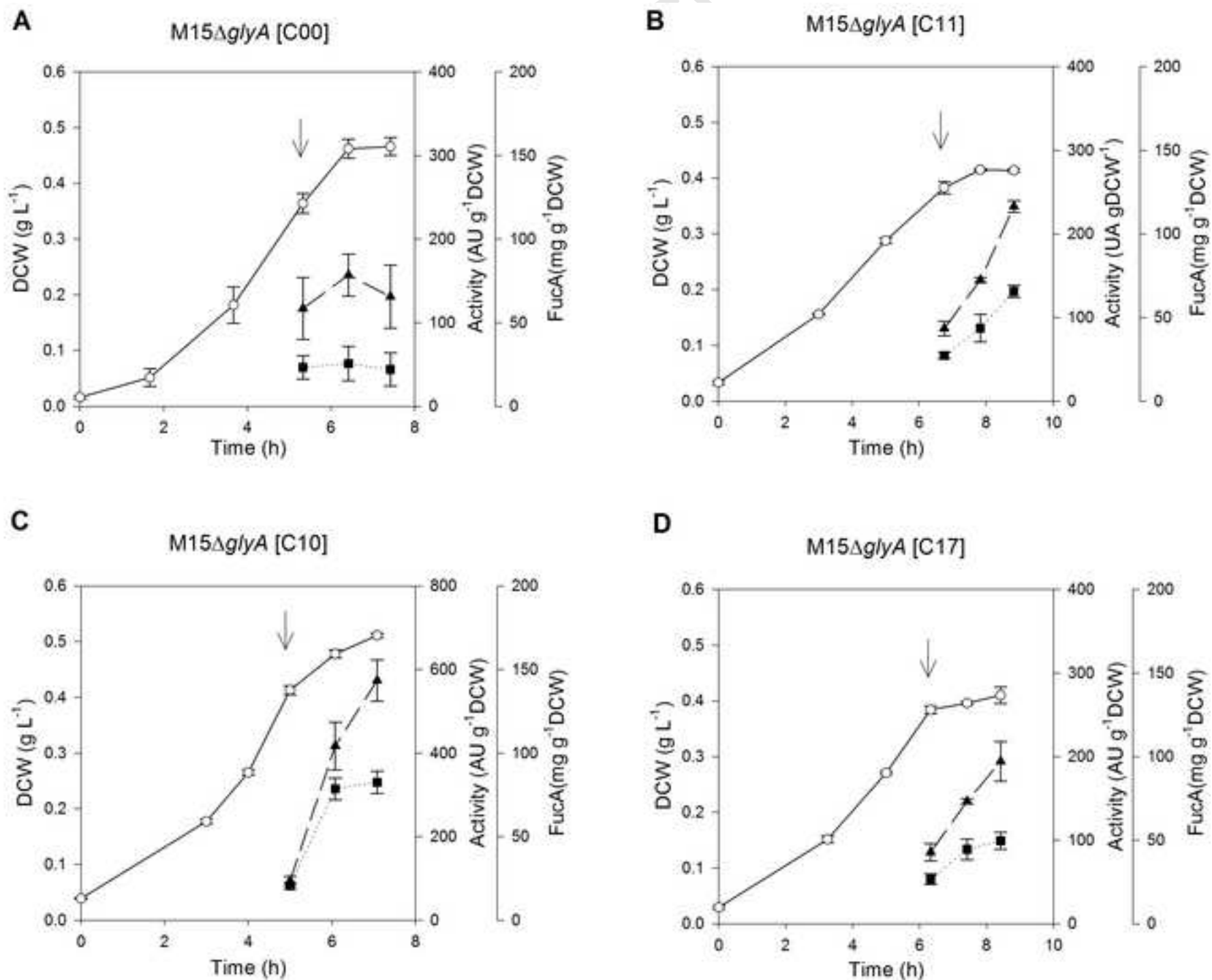


Figure 4

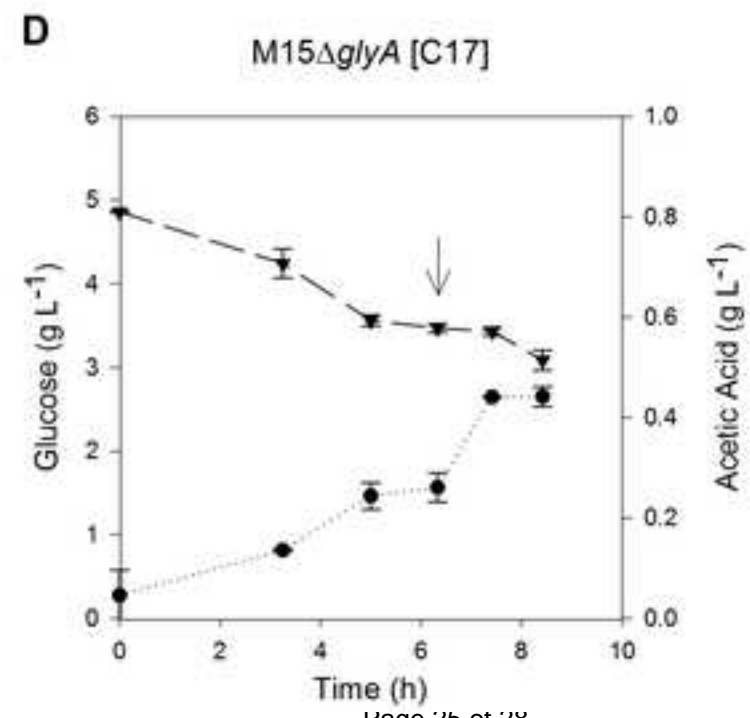
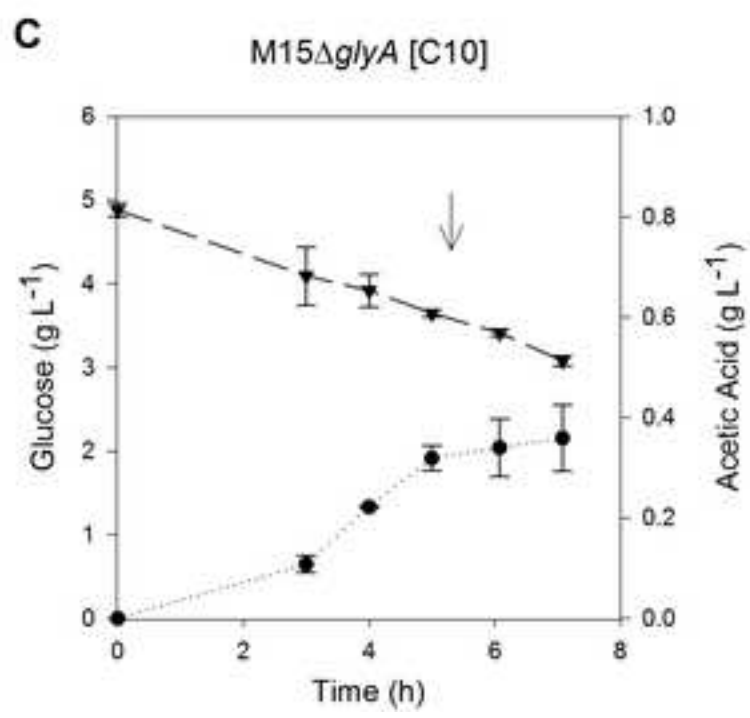
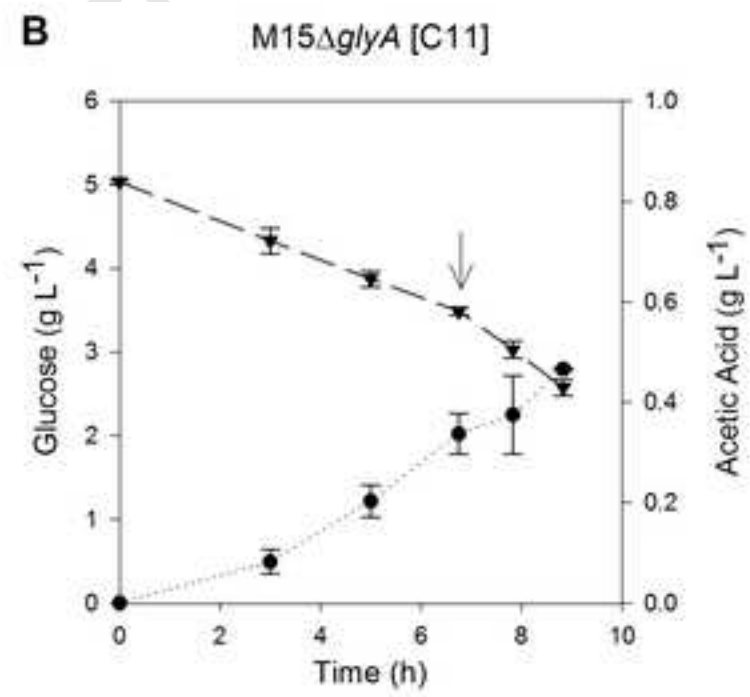
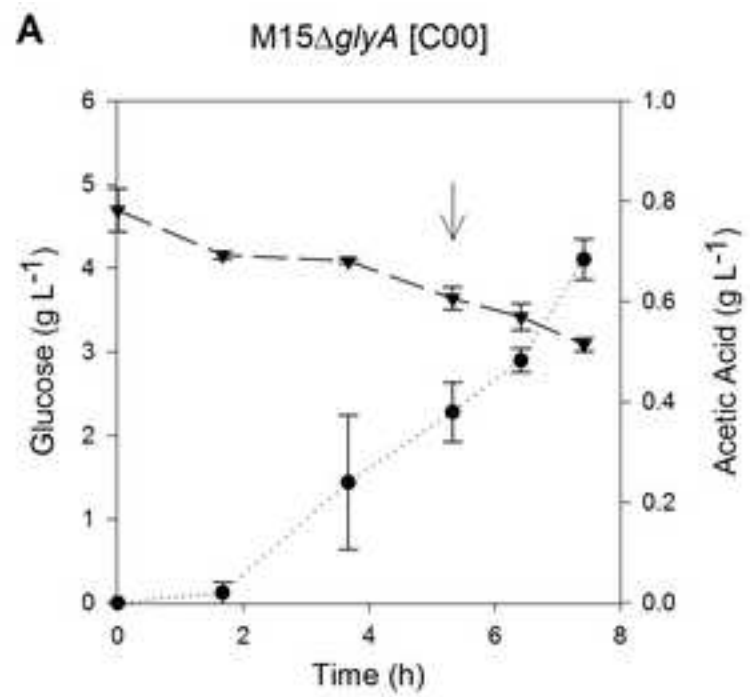


Figure 5

Manuscript

Puzzle

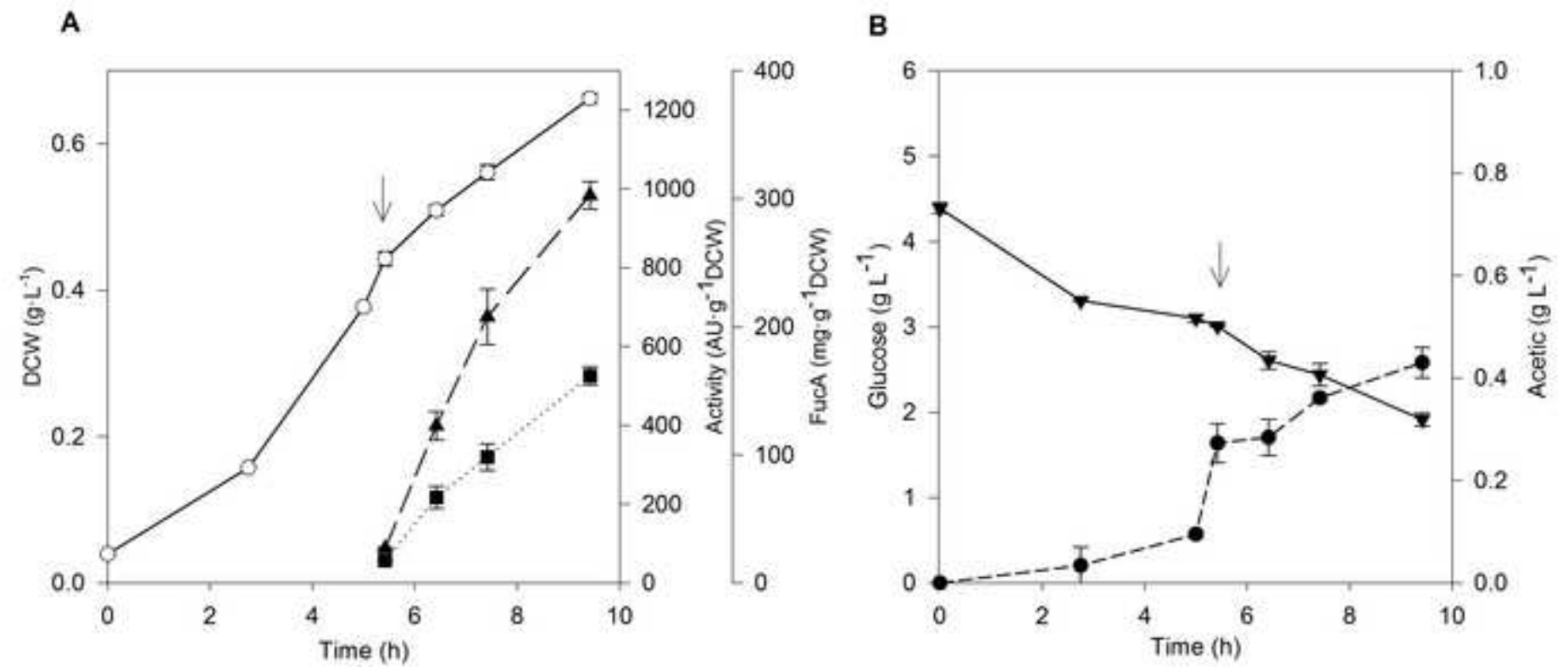
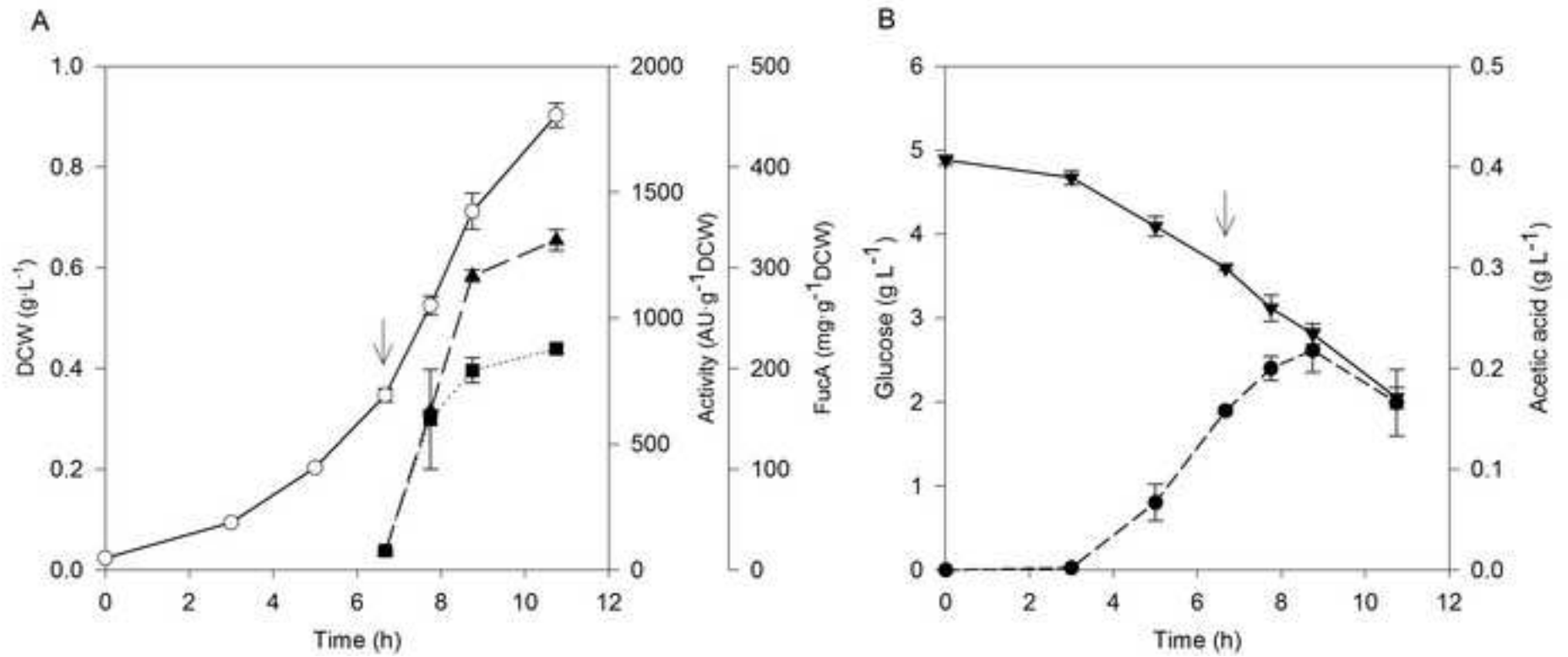
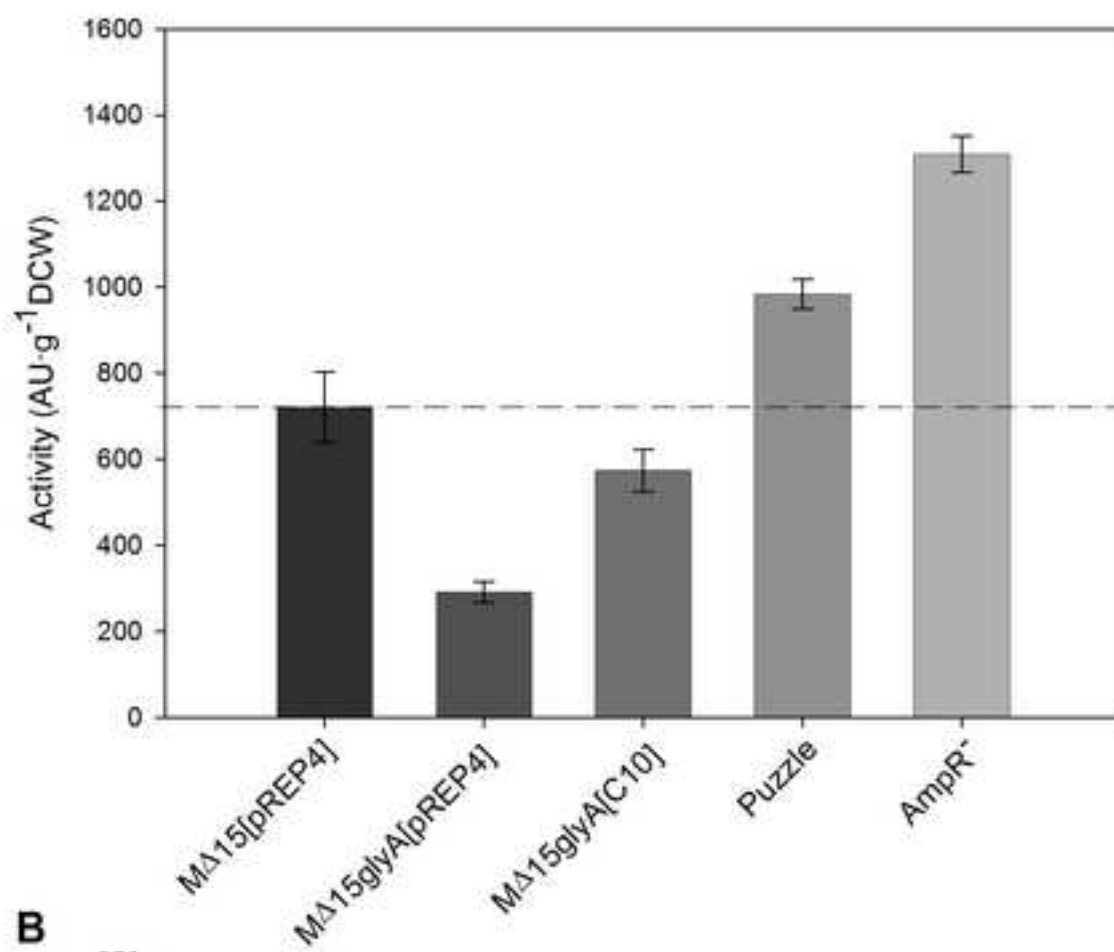


Figure 6

Manuscript

AmpR⁻



A**B**